STUDIES OF THE PULSE LINE ION ACCELERATOR*

W.L. Waldron, L.L. Reginato, E. Henestroza, LBNL, Berkeley, CA
A. Friedman, LLNL, Livermore, CA
R.J. Briggs, SAIC, Alamo, CA

Abstract

The Pulse Line Ion Accelerator concept was motivated by the need for an inexpensive way to accelerate intense short pulse heavy ion beams to regimes of interest for studies of High Energy Density Physics and Warm Dense Matter. A pulse power driver applied to one end of a helical pulse line creates a traveling wave that accelerates and axially confines the heavy ion beam pulse. The concept has been demonstrated with ion beams at modest acceleration gradients. Acceleration scenarios with constant parameter helical lines are described which result in output energies of a single stage much larger than the several hundred kilovolt peak voltages on the line, with a goal of 3-5 MeV/m acceleration gradients. This method has the potential to reduce the length of an equivalent induction accelerator by a factor of 6-10 while simplifying the pulsed power systems. The performance of prototype hardware has been limited by high voltage partial discharges across the vacuum insulator. Bench tests and analysis have led to significantly improved discharge thresholds. Further studies using a variety of experimental configurations are planned.

INTRODUCTION

The original concept of using a pulse line ion accelerator (PLIA) for inexpensive ion beam acceleration came from a workshop to explore the use of ion beams to heat matter to regimes of interest for studies of high energy density physics (HEDP) and warm dense matter (WDM). The combination of pulsed power and a helical slow-wave structure was an attractive concept in terms of simplicity and development and hardware costs compared to induction accelerators and large drift tubes. Further studies identified various operating modes and design considerations which proved this method to be particularly flexible [1]. This paper presents an overview of PLIA research whereas related papers at this conference present more details with regard to simulation efforts [2, 3].

SURFING MODE

In the surfing mode, a propagating ramped voltage waveform is launched down the PLIA at near synchronicity with an incoming ion beam. Appropriate design of the helix length, incoming ion velocity, and traveling wave speed can provide ideal trapping conditions, where the ion beam bunch, which is significantly shorter than the voltage ramp length, rides up and back down the ramp while in the helix such that the ions see an accelerating electric field for the entirety of their passage through the structure. Voltage waveforms can also be generated which simultaneously longitudinally confine or bunch the beam.

*Work performed under the auspices of the U. S. DOE by the University of California, LBNL Contract # DE-AC02-05CH11231 and LLNL Contract # W-7405-Eng-48.

SNOWPLOW MODE

In the snowplow mode, an ion bunch is fully loaded into the PLIA before the traveling wave is launched at a circuit speed which is faster than the ion beam velocity. The wave runs through the bunch such that the ions gain energy while they reside in the ramped portion of the waveform, and are bunched to a shorter physical length at the output. The ion beam bunch can be longer than the voltage ramp length, but less than or equal to the flattop portion of the voltage waveform (after bunching). By the end of the structure, the ions reside on the flat portion of the voltage waveform so that they can gain that additional energy as they pass through the termination resistor section. This concept using a PLIA is analogous to a "load and fire" system which uses a resistively graded high voltage column for injectors which require high initial line charge density. The beam is axially compressed because the particles in the tail of the beam are accelerated first, so they close the gap between the tail and the head before the head particles are accelerated (to the same final velocity).

DESIGN CONSIDERATIONS

As ions gain energy from the PLIA, they will ultimately outrun a traveling wave with a fixed velocity. This can be circumvented by tapering the impedance of the structure so that the wave speed increases with length. Although this would increase the final ion energy gain that can be achieved in a single PLIA section, the tapered PLIA is specific to a certain waveform and acceleration schedule. Fixed wave speed helices are simple to build and provide attractive flexibility for various experimental configurations.

Two approaches to driving the PLIA have been explored. One approach is to directly drive the upstream end of the helix, which looks like a high impedance transmission line. The advantage of this approach is that it requires very little current from the high voltage pulser and generating a wide range of waveforms is relatively easy. The disadvantage is that the high voltage feedthrough must handle the full helix voltage.

The other approach is to drive a primary strap which couples magnetic flux through the upstream end of the helix. With this approach, the primary to secondary (helix) coupling can be configured to give a step-up of voltage on the helix. Although the load for the pulser is very low impedance and generating a variety of waveforms is not trivial, the voltage requirement on the feedthrough can be a third or less of the full voltage.

INITIAL TESTING WITH BEAM

A successful proof-of-principle test and the corresponding simulations were performed with a 1 mA, 350 keV K+ beam [4]. The energy gain was measured with time-of-flight techniques as well as an electrostatic energy analyzer and compared to WARP simulations. Faraday cup data showing bunching was also compared to WARP simulations.

During the test, partial discharges in the vacuum were observed with an unusually low electric field threshold of < 2 kV/cm, as measured from the voltage waveform at the output resistive divider. This phenomenon was seen as a pressure burst in the vacuum system, visible light from the vacuum region, glitches and non-repeatability in the voltage waveforms, and significant loading of the accelerating waveform at the higher voltage levels. The experimental results with adequate pulse to pulse repeatability were obtained at a low enough voltage level that the effect of the partial discharge on the accelerating waveform was minimal. The effective acceleration gradient for this test was ~100 keV/m.

HIGH VOLTAGE TESTS

High voltage stress tests were done with a small Pyrex tube with vacuum on the ID which showed that there is not a fundamental electric field limitation below tens of kV/cm on the vacuum surface of a Pyrex tube. A peak gradient of 23 kV/cm was achieved with an undamped ringing voltage waveform (2-3 MHz) applied to a coil around the insulator. No visible light or pressure bursts were observed. The test was limited to these levels by the voltage capability of the pulser.

After the initial proof-of-principle beam tests, the indirect-drive oil PLIA was tested without beam to explore the partial discharge phenomenon which was limiting the acceleration gradient. To investigate the effect of attenuating the magnetic field at the vacuum surface of the insulator from the helix current, many closed rings were placed at the OD of the glass insulator. This modification did not improve the high voltage performance, but did lower the characteristic impedance and increase the wave speed from 1.9 m/us to 2.6 m/us.

To investigate a conceivable multipactor-like phenomenon, WARP was used to study possible electron trajectories which could lead to the discharges, but the results were inconclusive [5].

Previously, the only diagnostic which was available was the resistive voltage divider which was part of the termination resistor string. For this round of tests, capacitive pickups were placed along the helix structure to monitor the traveling wave and a current transformer was placed around the output of the high voltage pulser. Some experiments were also done with a high voltage probe looking at the input to the helix primary and a B-dot loop inside the glass tube. These additional diagnostics showed high frequency oscillations (28 MHz) on the helix primary and on the helix. This ringing could not been seen on the output termination resistive divider because of dispersion along the line at this frequency (Fig. 1). The minimum usable ramp length for this helix is ~100 ns (πa = 25 cm with a wave speed of 2.6 m/us). The capacitive pickups showed the amplitude of these oscillations decreasing quickly as the wave travels down the transmission line. A B-dot loop looking at B_z at the glass ID surface within the primary section of the helix showed the same 28 MHz (Fig. 2). The amplitude of this oscillation was significantly less at the center of the glass tube because fields at these high frequencies do not leak very far past the helix windings. It is almost certain that the helix and pulser used for proof-of-principle test with beam produced this same ringing, but the diagnostics were inadequate to observe the effect.

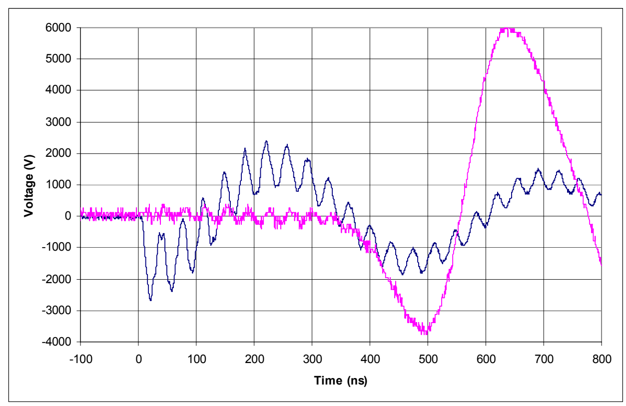

Figure 1: Blue trace is the primary voltage showing the 28 MHz oscillation. Magenta trace is the output voltage at the termination resistive divider showing a step-up of ~3. This low voltage test was without vacuum in the glass tube.

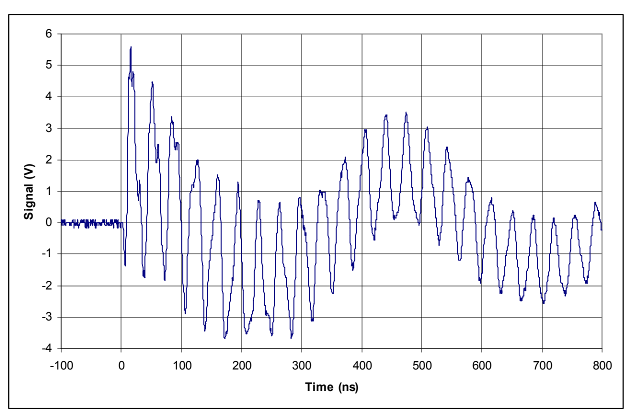

Figure 2: B-dot loop signal at the glass ID surface within the primary section of the helix showing the 28 MHz oscillation on B_z.

Modifications to the high voltage pulser (shorter output cable, filter network, and damping resistor) were implemented which decreased the amplitude and incidence of, but did not completely eliminate, the high frequency ringing in the drive circuit and the partial discharges. By using the output voltage waveform from the termination resistive divider and the capacitive probe signals, a peak voltage gradient of ~7 kV/cm and an average voltage gradient of ~6 kV/cm were demonstrated (Fig. 3, 4). Compared to the earlier tests, the partial discharge, which now occurred only intermittently (typically < 10% of the pulses), did not significantly load the traveling wave after these improvements in the pulser reduced the high frequency oscillations.

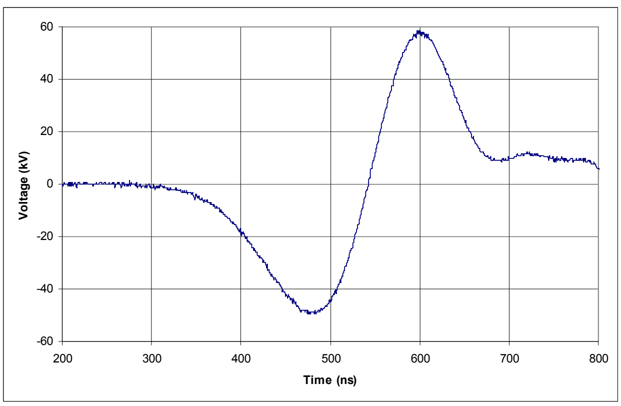

Figure 3: Output voltage at the termination resistive divider corresponding to ~6 kV/cm electric field.

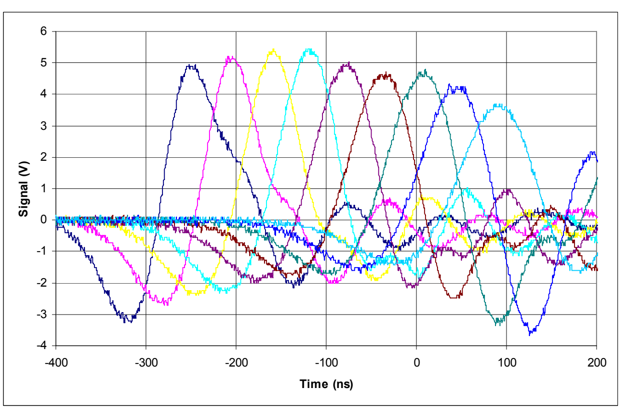

Figure 4: Signals from the capacitive pickups located every 10 cm along the PLIA to deduce the peak and average gradients when used with the termination resistive divider signal. The capacitive pickup signal is proportional to the time derivative of the voltage.

In the latest high voltage tests, a scaled direct-drive PLIA with a wave speed of 1.8 m/us has been fabricated which supports testing at faster ramp lengths and within existing high field solenoids (Fig. 5, 6) [6]. The oil PLIA mentioned above required very high voltages to explore gradients of interest because with an 8.1 cm radius helix, the minimum ramp length is around 25 cm (~πa) compared to 8 cm for the scaled PLIA. The oil PLIA was also too large to test within existing solenoids and the field geometry at the front end due to the transformer coupling complicated the partial discharge studies. A new pulser architecture was also implemented. Previously, all the pulsers had been capacitor spark gap discharge circuits which ring with the helix primary inductance. The voltage waveform using this method was very sensitive to stray inductance since the primary was such a low impedance (~600 nH). The new architecture is a tuned circuit with coupled inductors, which minimizes the effect of stray inductance, stray capacitance, and the 1.6 kOhm helix load on the voltage waveform.

Initial results from the scaled helix tests show 50 Mhz ringing on the pulser output current and frequent partial discharges (Fig. 7). Although the loading of the input and output voltage waveforms is negligible, the capacitive pickups show very strong indications of the partial discharges (Fig. 8, 9, 10, 11). These glitches on the capacitive pickups do not appear when there is no vacuum in the PLIA, so they are caused by the activity in the vacuum. For a given configuration of pulser and helix, the glitches occur at the same time in the waveforms and propagate at the nominal wave speed.

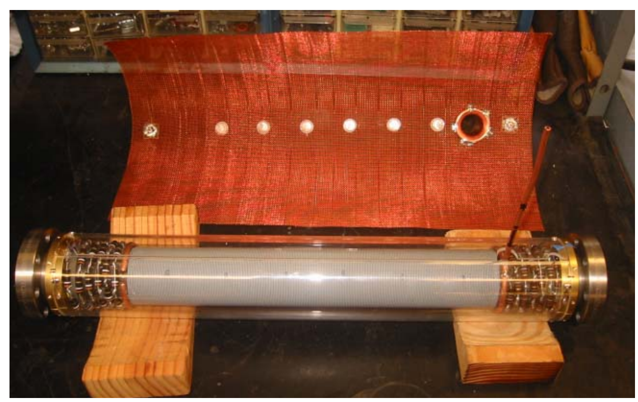

Figure 5: The scaled helix before the return shield has been wrapped around the gray insulated windings. The input and output resistive dividers can be seen as well as the 6 capacitive pickups underneath the shield. The total length of this assembly is 51 cm.

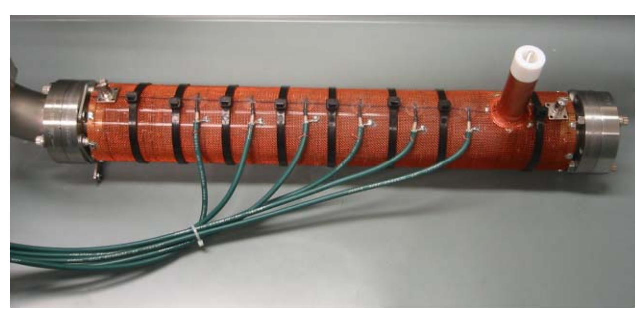

Figure 6: The scaled helix showing vacuum pumping from the left side and in a tank to be filled with dielectric oil. The direct drive high voltage feedthrough is on the right side with an exposed white Teflon insulator.

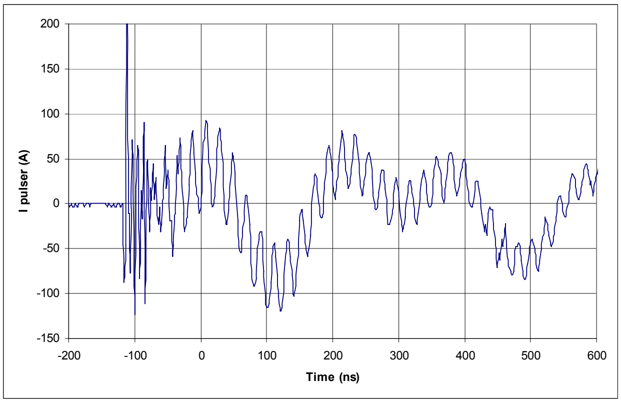

Figure 7: Pulser output current showing 50 MHz ringing.

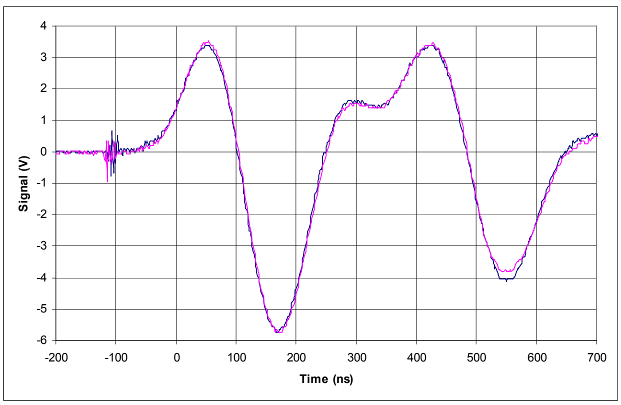

Figure 8: Blue trace is the raw helix input voltage divider signal without a partial discharge. Magenta trace is the raw helix input voltage divider signal with a partial discharge. The waveform differences are negligible. The calibration factor for this diagnostic is ~5 kV/V. The peak gradient is ~3.5 kV/cm.

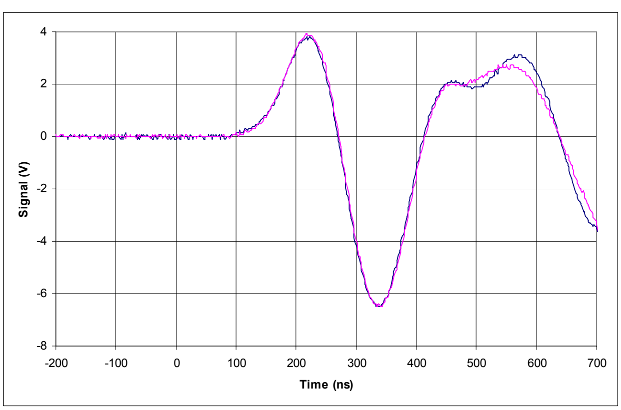

Figure 9: Blue trace is the raw helix output voltage divider signal without a partial discharge. Magenta trace is the raw helix output voltage divider signal with a partial discharge. The waveform differences are negligible. The calibration factor for this diagnostic is ~5 kV/V.

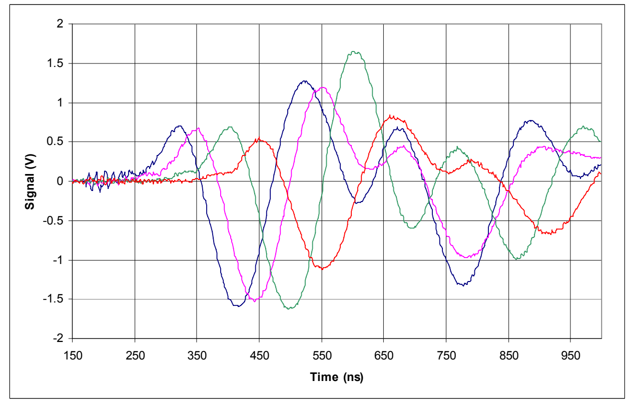

Figure 10: Capacitive pickups 1, 2, 4, and 6 without a partial discharge. Pickup 1 is closest to the helix input and pickup 6 is closest to the helix termination. The pickups are 5 cm apart.

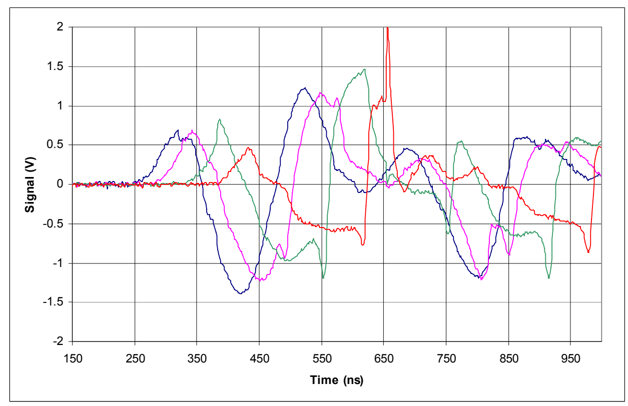

Figure 11: Capacitive pickups 1, 2, 4, and 6 showing glitches with a partial discharge. Pickup 1 is closest to the helix input and pickup 6 is closest to the helix termination. The pickups are 5 cm apart.

From these tests, we can conclude that the partial discharges are not exclusive to a particular input coupling field geometry (direct or indirect). We can also state that the glitches seen on the capacitive probes are the result and not the cause of the partial discharges. The next tests will attempt to characterize the structure as a load at different frequencies and to place a bandpass filter at the output of the pulser to eliminate any high frequency oscillations which are suspected to be the cause of the activity in the vacuum. Ultimately, we will test for gradient limits inside a solenoid which can produce up to 3T. All proposed applications of the PLIA require a high field solenoid for beam transport.

NDCX-II

Possible architectures for the second phase of the Neutralized Drift Compression Experiment (NDCX-II) are being studied at Lawrence Berkeley National Laboratory. The first phase (NDCX-I) has successfully demonstrated longitudinal and radial compression of a space-charge dominated K+ beam to ns pulse widths and mm spot sizes [7, 8]. This was achieved with a solenoid transport system, a bunching induction module, and a volumetric plasma source to neutralize the beam and overcome space charge forces. Initial WDM experiments are planned [9]. The purpose of the second phase is to use the same technique for HEDP and WDM studies which require more energy deposited on the target.

As an option for NDCX-II, the PLIA is being considered to do the initial longitudinal beam compression and acceleration. The high voltage performance needs to be better characterized, but the advantage of the PLIA is its simplicity and expected reduced cost compared to induction cells. Induction cells and Blumleins from the Advanced Test Accelerator (ATA) accelerator at LLNL are available for NDCX-II, but they were designed for 70 ns pulses at 250 kV [10]. To get the total required charge for significant HEDP experiments from known ion sources, the beam pulse width has to start at several hundred ns. To utilize the ATA hardware with minimal modification, the initial injector pulses need to be compressed to < 70 ns. This longitudinal compression can be achieved with multiple induction cells or a single untapered PLIA operating in the snowplow mode. The multiple induction cell approach requires various ramped voltage waveforms which makes the use of the original ATA Blumleins problematic. New pulsers would likely need to be designed and fabricated. The PLIA approach is attractive because the slow-wave structure is simple to fabricate and only one high voltage pulser is required, but the larger solenoid does introduce some cost

Two possibilities using the PLIA are being explored using WARP to model the beam dynamics. In the first scenario, the goal of the PLIA is to compress and accelerate the beam to 750 keV, which is the output energy of the beam from a solution using only induction cells. This results in a 3.5 m PLIA with an acceleration gradient of ~200 keV/m. Acceleration with a bunch this long is inherently low gradient and not a particularly attractive solution. In the second scenario being studied, the goal of the PLIA is to bunch the beam as quickly as possible, while preserving the emittance, so that the acceleration can then be done with the ATA induction cells and Blumleins which are available and would be used at a derated acceleration gradient of 700 keV/m. For the front end of this machine, the voltage gradients required to do bunching and minimal acceleration are levels that have been demonstrated. A PLIA for acceleration of the 70 ns pulse can be considered after the acceleration gradient has been demonstrated at $\geq$ 1 MeV/m.

CONCLUSION

Both direct and indirect drive helical pulse lines have been fabricated to investigate the engineering limits of the PLIA. Recent tests have resulted in useful electric field gradients with minimal loading of the traveling wave, but partial discharges in the vacuum system still occur intermittently. We believe that the high frequency ringing from the spark gap based drive pulser is the most likely cause of these partial discharges, and means for further reduction of this ringing will be explored. In addition, variations in an applied axial magnetic field, the applied voltage waveform (and pulser architecture), and grading ring configuration will be used to attempt to suppress these partial discharges. Because we have demonstrated beam bunching and acceleration, and have attained useful gradients with minimal loading of the traveling wave, studies will continue to look at applications of the PLIA for bunching and acceleration in NDCX-II.

REFERENCES

[1] R. J. Briggs, "Pulse Line Ion Accelerator Concept," PRST-AB **9**, 060401 (2006).

[2] A. Friedman, *et al.*, "Modeling of the Pulse Line Ion Accelerator (PLIA): An Algorithm for Quasi-static Field Solution," these *Proceedings*.

[3] E. Henestroza, "Electromagnetic Simulations of the LBNL Pulse Line Ion Accelerator (PLIA) Experiments," these *Proceedings*.

[4] P.K. Roy, *et al.*, "Energy Amplification and Beam Bunching in a Pulse Line Ion Accelerator," PRST-AB **9**, 070402 (2006).

[5] J.E. Coleman, *et al.*, "Beam Experiments on the Pulse Line Ion Accelerator," NIM A 577, 197-202 (2007).

[6] A. Friedman, "A Scaled Helix for Breakdown Studies," LLNL Report UCRL-TR-224518-REV-1 (2006).

[7] P.K. Roy, *et al.*, Drift Compression of an Intense Neutralized Ion Beam," PRL **95**, 234801 (2005).

[8] J.E. Coleman, *et al.*, "Bunching and Focusing of an Intense Ion Beam for Target Heating Experiments," these *Proceedings*.

[9] F.M. Bieniosek, *et al.*, "Experiments in Warm Dense Matter using an Ion Beam Driver," these *Proceedings*.

[10] L.L. Reginato, "The Advanced Test Accelerator (ATA), a 50-MeV, 10-kA Induction Linac," *IEEE Trans. on Nuclear Science*, Vol. NS-30, No. 4, 2970-2974 (1983).

1-4244-0917-9/07/$25.00